2

Exploring Plastic Deformation of Metallic Materials by the Acoustic Emission Technique

Kristián Máthis and František Chmelík
Department of Physics of Materials, Faculty of Mathematics and Physics, Charles University, Prague, Czech Republic

1. Introduction

In determination of direct correlation between material properties and parameters of testing environment, the non-destructive *in-situ* methods play an important role. Non-destructive experimental techniques facilitate correlation of material parameters to those of the testing environment in real time. Among the tools emerging in the last decades, the acoustic emission (AE) technique belongs to the most powerful and reliable ones. The AE method allows to determine, which external parameters are critical for behaviour of the investigated material. Thus the results of AE measurements could give an integral hint for further *post mortem* investigations (e.g. scanning or transmission electron microscopy), in which the material properties are evaluated just after the exposure of the specimen to the external environment.

The AE is generally defined as elastic energy spontaneously released during local, dynamic and irreversible changes of the (micro)structure of the materials. Various nature phenomena as earthquake, avalanche, landslide or crack propagation in ice cover are accompanied by AE. Therefore it is often called in non-professional terminology as "the sound of the danger". AE is also observed during plastic deformation and phase transformations in materials. Another kind of AE appears during leak testing, when not the material itself, but the fluid or gas leakage generates detectable sound waves.

This chapter is focused on AE occurring during plastic deformation of metallic materials. In this case, it responds to dislocation motion and twinning and therefore yields information on the dynamic processes involved in plastic deformation of metals and alloys. The first documented observation of AE in metals is the so-called tin cry, the audible AE produced by mechanical twinning of pure tin. After the pioneering works of Czochralski (Czochralski,1916) and Joffe (Joffe,1928) from 1920s, the systematic investigation of the AE phenomenon started just after the World War II. In 1948, Mason and his co-workers observed intensive AE signals in a wide frequency range during deformation of thin tin plates. The most important milestone in the history of the AE was the PhD work of Josef Kaiser in 1950 dedicated to the systematic study of AE during forming of various metallic and non-metallic specimens (Kaiser,1950). He described typical AE response of several metallic materials and discovered the irreversibility phenomenon, which is called the *Kaiser-effect*. In 1957, Clement A. Tatro formulated the two main tasks of the AE research: (1)

discovering the physical background of the AE; (2) developing AE systems for industrial use (Tatro,1957). The latter task was fulfilled first by Harold L. Dunegan in 1963, who tested safety of pressure vessels by the AE technique (Dunegan,1963). Thanks to the fast progress in semiconductor industry, the number of the industrial applications in last three decades increased dramatically.

2. Principles of acoustic emission monitoring

The AE permits real-time monitoring of structural changes in the investigated material. Nevertheless, the interpretation of the results is often difficult. To this very day it does not exist an exact theory for characterization of AE, since the description of AE sources and the wave propagation sets a lot of unsolved mathematical problems. All the same works of Lord (Lord,1981) and Vinogradov (Vinogradov,2001) foreshow the possible way of solving at least some model situations. Fortunately, the combination of the outputs of AE experiments and the cognitions about the materials' structure resulted in several empirical and semi-empirical models that give a guideline for the everyday AE practice.

2.1 Features of the acoustic emission signals

The detection of AE is based on its physical nature, namely the elastic energy release due to some irreversible change of the (micro)structure. Near the AE source, the released energy forms a stress pulse, which propagates through the material bulk as transient elastic waves. Depending on the geometrical configuration and the dimensions of the specimen, the stress pulse is transformed into a specific wave mode. The wave component perpendicular to the surface may be detected by piezoelectric transducers, which are coupled to the specimen surface either mechanically or through a waveguide. Electrical signal from the transducer is first preamplified and then led to the input of the measuring system, where it is again amplified and analysed. Obviously, the waveform of the AE signal is significantly affected by the source mechanism, propagation through the specimen volume and detection by the transducer.

Principally, two basic types of AE signals can be recognized. In the case of the *continuous signal*, the amplitude does not fall under a certain threshold level during relatively long period of time. The continuous signal is connected with micromechanisms of plastic deformation (e.g. dislocation glide (Heiple&Carpenter,1987a, Heiple&Carpenter,1987b)) and relaxation of large internal stresses (recrystallization, phase transitions etc.). A number of spurious signals have also continuous character, as friction or machine noise. On the contrary, the *discontinuous signals* (also called as *discrete* or *burst type* AE) are distinctly separated in time. Their generation is avalanche-like and the released energy is by several orders larger than that of continuous signal. Characteristic sources of discontinuous signals are nucleation of twins, crack initiation and propagation or corrosion processes. Stephen and Pollock (Stephens&Pollock,1971) assumed a pulse character of elastic waves in discontinuous signal and a step-like movement of the elementary parts of the material. They described the spectral distribution of the AE energy as follows:

$$A(f) = \frac{y_0^2 E}{c_L} \exp\left(-\frac{(2\pi f\, T)^2}{2}\right), \tag{1}$$

where y_0 is the displacement of the elementary volume of the material due to the stress impulse, E is the Young 's modulus, c_L is the longitudinal sound speed, f is the frequency and T is the duration of the pulse. This equation results in a normal distribution and describes well the experimental results.

The continuous signals were long time considered as a result of overlapping discontinuous signals. The study of Hatano (Hatano,1975) first showed, that the continuous signal reflects a sum of random AE pulses.

2.2 Basic terms and parameters of acoustic emission signals

The *AE event* is a single dynamic process releasing elastic energy. The local process producing AE event is called the *AE source*. The electric signal detected at the output of the transducer is termed the *AE signal*.

The AE measurements are usually carried out in the presence of continuous background noise. Therefore a *threshold level* is set in order to filter out the signal noise.

In case of *discontinuous signal* every AE event is evaluated separately. The onset of the AE event is characterized by time t_s, when the AE signal first exceeds the threshold level (Fig. 1). The end of the event could be defined by using a *dead-time* t_d (*hit definition time – HDT* in Physical Acoustic Corporation devices). The time of the AE event termination t_e is set in, when the signal did not exceed the threshold level during the last t_d period. The *duration* of the event is defined as $t_e - t_s$.

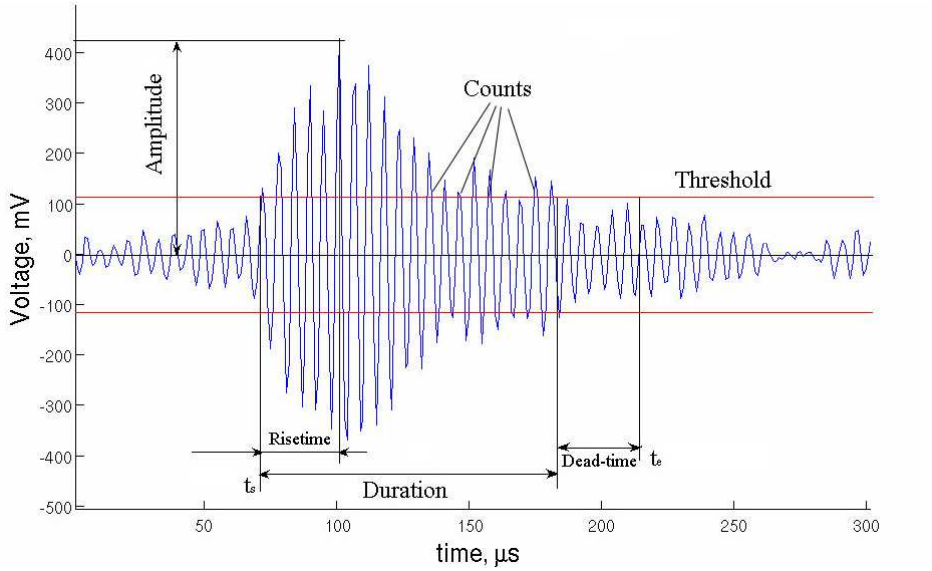

Fig. 1. Definition of discontinuous signal parameters.

The parameters of the discontinuous AE signal are the following (Fig. 1):

- *Amplitude* – maximum amplitude of the signal during its duration

- *Rise time* – time elapsed between the onset of the event and achieving the maximum amplitude.
- *Count* - the number of times the AE signal exceeds the threshold level
- *Duration* – the definition see above
- *Event energy* – is the area under the acoustic emission waveform. Usually, the evaluation systems calculates the electrical energy, defined as follows:

$$E = \frac{1}{R}\int_{t_s}^{t_e} V^2(t)dt\,, \tag{2}$$

where R is the electrical resistance of the measuring set up, V is the measured voltage and t is the time.

Cumulative representation of these parameters could be also defined, e.g. cumulative counts or cumulative energy.

The *continuous signal* is mostly evaluated in terms of the root *mean square value (RMS)* of the signal voltage and the *count rate* – the number of threshold crossings per a time unit.

Since the reliability of the AE measurements is very sensitive to the proper setting of the set up parameters (threshold, dead-time), the up-to-date AE systems enable continuous sampling and storing of AE signal, so-called data streaming. In this case the controlling computer acquires the raw data for later evaluation by the operator. The advantage of this approach is that it avoids any data loss due to incorrect system settings. Furthermore, the evaluation parameters could be fit more precisely. On the other hand, the data files are large (~1 Gb/min), which requires long computing time during the post-processing.

3. Microscopic origin of acoustic emission during plastic deformation of metals

The AE method is suitable for monitoring of collective dislocation motion, as well as for the investigation of deformation twinning. Both processes are associated with the dislocation dynamics, and they are significant sources of AE (Heiple&Carpenter,1987a). Therefore it is essential to understand the physical background of the AE generation by dislocations.

3.1 Dislocation model of acoustic emission

The dislocation model of AE has to include several key paragraphs. First of all it is necessary to identify the processes that generate AE. The aspects of the AE detection should be also discussed.

Hirth and Lothe (Hirth&Lothe,1982) have shown that a dynamic stress field has to exist in the material, when AE is generated. There are three basic dislocation mechanisms (Heiple&Carpenter,1987a) generating AE:

- *Relaxation of stress field caused by passage of dislocations* – the transient part of stress field of a moving dislocation causes AE.
- *Annihilation of dislocations* – disappearance of stress fields of annihilated dislocations causes AE

- *Bremsstrahlung* – acoustic radiation of accelerated (decelerated) dislocations

In practice, during the AE experiments the surface displacement is detected . Therefore it is essential to estimate the magnitude of the surface displacement produced by dislocation passage. The simplest configuration, i.e. surface displacement Δu from a longitudinal wave caused by growing dislocation loop in an isotropic sample, was calculated by Scruby et al. (Scruby,1981). They assumed a growing dislocation loop lying in depth D below the surface under angle 45° to the surface normal. If it reaches a maximal radius r at a constant growing velocity v, the maximal displacement can be written as:

$$\Delta u = \frac{brc_T^2}{Dc_L^3}, \tag{3}$$

Where b is the Burgers vector, c_L and c_T are the longitudinal and transversal wave speeds, respectively. Heiple and Carpenter (Heiple&Carpenter,1987a) calculated the maximal displacement in an aluminum single crystal with 4 mm in diameter. The substitution of typical values (c_L = 6400 ms^{-1}, c_T = 3200 ms^{-1}, D = 4 cm, b = 0.29 nm, v = 200 ms^{-1}) yielded a displacement of Δu = 10^{-13} m. Despite of the fact that the sensitivity of sensors are of the order of 10^{-15} m (Miller&Hill,2005), such a displacement is hardly detectable. In a real crystal, where the dislocation movement is hindered by various obstacles (grain boundaries, stress field of other dislocations etc.), the maximal surface displacement decreases by several orders (Heiple&Carpenter,1987a). Thus it could be concluded, that the signal generated by a single dislocation loop is not detectable.

The production of AE by annihilation of dislocations was investigated in several studies by Natsik et al. They investigated mechanisms of passing of dislocations at the surface (Natsik&Burkanov,1972), annihilation of moving dislocations (Natsik&Chishko,1972) and the activity of Frank-Read sources (Natsik&Chishko,1975, Natsik&Chishko,1978). Instead of assuming maximal surface displacement, they compared the amount of released energy as a consequence of annihilation of dislocations and the change of the grain shape caused by moving dislocation, respectively. The released energy caused by annihilation of a dislocation pair was set as (Natsik&Chishko,1972):

$$E_{an} = (\rho b^2 u^2 / 8\pi)\gamma \ln d / b, \tag{4}$$

where ρ is the density of the material, u is the velocity of the dislocations in the moment of the annihilation (in the original paper $u = 0.1 - 1\, c_T$ is recommended), γ = 1 for screw dislocations and $1 + (c_T / c_L)^4$ for edge dislocations, and d is the grain size. In case of Al crystal (ρ = 2700 kg m^{-3}, u = 1600 m s^{-1}, d = 80 μm) we get E_{an} = 2.9 × 10^{-10} J m^{-1}. According to Tetelman (Tetelman,1972) the released energy during deformation of a cube-shaped grain (d is the size of the cube's edge) caused by dislocation motion could be written as:

$$E_g = b\tau d, \tag{5}$$

where τ is the applied stress. For Al single crystal (τ = 4 MPa) E_g = 9.3 × 10^{-8} J m^{-1}. It means that during the dislocation annihilation the released energy is approximately three hundred times smaller than that for dislocation slip.

The *bremsstrahlung* was studied first by Eshelby (Eshelby,1962) and Kosevich (Kosevich,1964), who investigated oscillating dislocations (Eshelby,1962) and accelerating dislocation groups (Kosevich,1964). Kiesewetter and Schiller (Kiesewetter&Schiller,1976) described the nucleation, moving and pinning of dislocations as a periodic process, whose maximal amplitude is given by the distance source – pinning site. The radiated energy per second of a screw dislocation having an oscillation frequency of $\omega_0 / 2\pi$ is:

$$P_B = \frac{Gb^2 l^2 A_d^2 \omega_0^4}{20\pi c_T^3}, \tag{5}$$

where G is the shear modulus, l is the length of the dislocation line, $A_d = 2\pi v/\omega_0$ is the moving amplitude, v is the velocity of the dislocation. Again for Al, where $G = 2.64 \times 10^4$ MPa, $l = 80$ μm, $A_d = 40$ μm, $\omega_0 = 2\pi v/A_d = 3.1 \times 10^7$ s^{-1}, the value of $P_B = 10^{-8}$ W. Consequently, the bremstrahlung energy radiated during one period is:

$$E_B = \frac{2\pi P_B}{1\omega_0} = 5 \text{x} 10^{-11} \text{Jm}^{-1}. \tag{6}$$

This value is even smaller than that for dislocation annihilation.

According to the described results it can be concluded that the AE generated by a single dislocation is not detectable. Thus, the occurrence of detectable AE during deformation of metallic materials indicates a cooperative character of dislocation motion. In virtue of equations (3)-(5) it can be predicted that at least 100 moving dislocations or 10000 concurrent annihilations of dislocation pairs are necessary for generating detectable AE. Naturally, that is true only ideally, since part of the released energy is transformed to heat due to different interactions (e.g. with phonons) and another part is lost without being detected. Heiple and Carpenter (Heiple&Carpenter,1987b) and Gillis and Hamstad (Gillis&Hamstad,1974) estimated the part of the released energy, which will transfer to detectable AE to 0.7% and 1%, respectively,. However, as the number of dislocations in the pile-ups is very large, the detection of AE at proper conditions is possible. Sedgwick (Sedgwick,1968) assumed that the fast operating dislocation sources and the sudden release of dislocation pile-ups are in the background of detectable AE.

James and Carpenter (James&Carpenter,1971) investigated several parameters of plastic deformation of LiF crystals, as increment of dislocation density, increase of density of the mobile dislocations and changing rate of the density of the mobile dislocations. They demonstrated that the AE event rate is proportional to the change in the density of the mobile dislocations, i.e. it is connected with the conversion of immobile dislocations to the mobile ones. They proposed an avalanche-like dislocation breakaway model, in which the dislocations are pinned at obstacles. The increasing stress and/or the thermal activation cause breakaway of several dislocations. This process actuates a stress wave that causes further dislocation de-pinning. Finally, an avalanche-like process arises, accompanied with an intensive stress pulse.

Agarwal et al. (Agarwal,1970) examined the second AE source mechanism proposed by Sedgwick (Sedgwick,1968), i.e. the fast multiplication of dislocations. They assumed that the AE is generated, when the deformation stress reaches the value necessary for

activation of the first dislocation source. Subsequently, the dislocations nucleate fastly and move towards the next obstacle. According to their estimation in case of 100 μm² large dislocation free area nucleation of at least 0.01 cm long dislocation line is necessary for generation of detectable AE.

The internal friction model worked out by Granato and Lücke (Granato&Lücke,1956) could reveal, which further mechanisms are linked with AE. The amplitude independent part of the damping curve is proportional to the fourth power of the average dislocation loop length between the pinning points and directly proportional to the dislocation density. It can be concluded that the dislocation breakaway process, which raises the average dislocation length increases the internal friction more than the dislocation generation. Thus a concurrent measurement of internal friction and AE could clarify , whether the breakaway or the dislocation multiplication process is the dominant AE source (Heiple&Adams,1976, Higgins&Carpenter,1979).

In practice, the above described processes will likely contribute to AE concurrently which makes difficult to distinguish between them.

3.2 Acoustic emission response of twinning activity

Twinning, which is a deformation mechanism observed mostly in structures with lower symmetry (e.g. hexagonal closed packed, hcp, structure) belongs to the first identified sources of AE. Even though, there has been no model describing this process in detail. Assuming the mechanisms discussed in the §3.1 we could attempt a rough approximation. It could be suggested that the source mechanisms of AE during twinning are relaxation of stress fields in the crystal and the bremsstrahlung, respectively. A pole mechanism for twin formation in hcp structures was proposed by Thomson and Millard (Thompson & Millard, 1952), who suggested the following dislocation reaction to form a pole source of twinning:

$$\left[0001\right] \rightarrow \alpha\left[10\bar{1}0\right] + \left[10\bar{1}0\right], \tag{7}$$

where α is a small fraction, ranging from 1/12 to ¼. This mechanism is in essence a modification of the Frank-Read source; only the rotating edge dislocation is replaced by a twinning one. The Thomson-Millard source reels off twinning dislocations, which are accelerated by local stresses to supersonic speed. This process causes similar surface displacement as a dislocation loop described by Eq. (3). Even a single twin dislocation (r = 40μm – the average length of twins are comparable with the grain size, v = 2000 ms^{-1}) produce a detectable surface displacement of $\Delta u = 10^{-14}$ m. Furthermore, the twin nucleation is a result of collective motion of several hundred dislocations. Thus, it is not surprising that the twin nucleation is a significant AE source. On the other hand, the twin growth does not generate detectable AE. Since the growth velocity of an elliptical twin is in order of 10^{-3} ms^{-1} (Papirov,1984), the surface displacement caused by twin growth is only $\Delta u = 5 \times 10^{-22}$ m. Carpenter and Chen (Carpenter&Chen,1988) proved experimentally the above mentioned theory. During deformation of zinc single crystal they found a strong correlation between the number of AE events and the number of twins. Furthermore, they clearly pointed out that the contribution of the twin growth is negligible compared to the twin nucleation.

3.3 Intensity of acoustic emission signal

As discussed above, there are numerous processes during plastic deformation that can generate AE. Their efficiency is summarized in Table 1.

Mechanism of plastic deformation	Strength of AE signal
Frank-Read source	strong
Twin nucleation	strong
Yield phenomenon	strong
Cutting of coherent precipitates by dislocations	strong
Orowan bowing	weak
Twin growth and thickening	negligible
Grain boundary sliding without cracking	negligible

Table 1. Intensity of AE signal due to various processes of plastic deformation

Generally, the AE signal is influenced by various experimental parameters: e.g. crystal structure, grain size, preferred crystal orientation, solute alloying, phase composition and structure, mechanical work history; strain rate, testing temperature, testing environment and irradiation. In the following chapters, the influence of some of these parameters on the AE response will be discussed in detail for various materials with hexagonal closed packed structure

4. Acoustic emission measuring system used in our experiments

In the experiments described in the following chapters the DAKEL-XEDO-3 AE facility by the DAKEL-ZD Rpety, Czech Republic was used. The AE signal was acquired at sampling rate of 4 MHz and evaluated in real time using a two threshold level detection. This procedure yields a simple amplitude discrimination and two AE count rates (Count rate at level 1 and Count rate at level 2). As the first threshold level was set directly above the peak values of noise, the AE count at this level was assumed to be the sum of the response of all deformation mechanisms detectable by AE. The burst AE count, measured at the second threshold level, was used for gathering signals coming from strong effects (e.g. twinning).

5. Acoustic emission during plastic deformation of magnesium alloys and composites

Magnesium-based alloys, as one of the lightest structural materials, have been the focus of researchers' and engineers' interest for many years. Their unique properties - such as high specific strength (the ratio of the yield stress to density), superior damping capacity and high thermal conductivity - predetermine these materials for use in many structural applications, such as in the automotive and aerospace industries. The main restriction to a wider use of magnesium alloys is their limited ductility and poor formability at ambient temperature, poor creep and corrosion resistance, and a degradation of their mechanical properties at higher temperatures (above 200°C) (Avedesian&Baker,1999). Part of the above listed disadvantages can be eliminated by using Mg-based metal matrix composites (MMCs), e.g. creep resistance or high temperature stability (Sklenicka&Langdon,2004, Trojanova,2010). The microstructure and mechanical properties of MMCs are influenced significantly by the interfaces between the

matrix and the reinforcement. When a MMC is submitted to temperature changes (cooling down from the temperature of fabrication, cyclic temperature changes during operation of structural parts) thermal stresses arises at the interfaces owing to a considerable mismatch of the thermal expansion coefficient of the matrix and that of the reinforcement. Thus the right choice of processing and operating temperature of Mg-based MMCs is a key question.

The poor ductility of magnesium is due to its hexagonal closed packed (hcp) structure. In hcp metals there are three main slip systems (Fig. 2): basal, prismatic and pyramidal of first and second order.

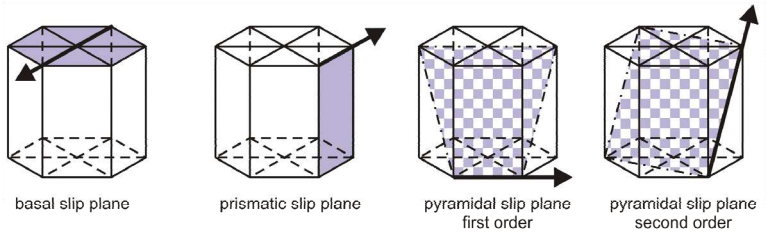

Fig. 2. Main slip systems in the hexagonal-closed packed structure

The mechanisms of plastic deformation significantly depend on the ratio of crystallographic axes *c/a*. If this ratio is larger than the ideal value of $\sqrt{8/3}$ (Zn), the basal plane has the largest atomic density and the basal slip will dominantly operate . If the *c/a* ratio is smaller than $\sqrt{8/3}$ (e.g. Ti), the primary slip occurs in the prismatic and pyramidal planes. Magnesium belongs to the third group, since its *c/a* ratio is nearly ideal. Therefore in certain cases the basal slip could be replaced by pyramidal or prismatic slip. The activation of non-basal systems depends on several parameters, e.g. on alloying content or testing temperature.

As it was shown first by von Mises (von Mises,1928), the activation of at least five independent slip systems is necessary for homogeneous plastic deformation of polycrystals. The slip systems in hcp metals are summarized in the Table 2.

	Burgers vector	**Slip direction**	**Slip plane**	**Independent slip system**
Basal	***a***	$\langle 11\bar{2}0 \rangle$	(0001)	2
Prismatic 1st order	***a***	$\langle 11\bar{2}0 \rangle$	$\{10\bar{1}0\}$	2
Pyramidal 1st order	***a***	$\langle 11\bar{2}0 \rangle$	$\{10\bar{1}1\}$	4
Pyramidal 2nd order	***c + a***	$\langle 11\bar{2}3 \rangle$	$\{11\bar{2}2\}$	5
Prismatic 1st order	***c***	$\langle 0001 \rangle$	$\{10\bar{1}0\}$	2
Prismatic 2nd order	***c***	$\langle 0001 \rangle$	$\{11\bar{2}0\}$	2

Table 2. Slip systems in the hexagonal closed-packed materials

As it is evident from the Table 2, the basal and prismatic systems provide only a total of four independent slip systems; none of them can produce a strain parallel to the *c*–axis. It is clear that the activation of second order pyramidal slip system is necessary for plastic deformation. Nevertheless, the size of the Burgers vector of the ***c + a*** slip is large in comparison to the interplanar crystal spacing, therefore the dislocation width is small and its gliding is difficult (Hutchinson,1977). The ***c + a*** dislocations were extensively studied in single crystals (Ando&Tonda,2000, Blish&Vreeland,1969, Obara,1973, Paton&Backofen,1970, Stohr&Poirier,1972). Generally, it could be concluded that the critical resolved shear stress (CRSS) for the second order pyramidal slip system decreases with the increasing temperature. Nevertheless, in case of magnesium single crystal, the results are ambiguous (Ando&Tonda,2000, Chapuis&Driver,2011, Obara,1973, Stohr&Poirier,1972). The reason could originate from the inaccuracy of the crystal orientation alignment. If the orientation difference between the *c*-axis of the crystal and the direction of the applied stress is larger than 5 angular minutes, the basal slip and twinning disturb the measurement (Stohr&Poirier,1972). However, the latest electron backscatter diffraction (EBSD) measurements (Chapuis&Driver,2011) show a monotonic decrease of CRSS for the ***c + a*** slip with temperature.

There are only limited data about pyramidal slip in magnesium polycrystals. Agnew and his co-workers investigated Mg-Li alloys by means of transmission electron microscopy (TEM) and X-ray diffraction (Agnew,2001). They found that the Li addition decreases the CRSS of the pyramidal slip and the ***c + a*** dislocation could be activated already at room temperature. Detailed study of temperature dependence of the ***c + a*** slip activity in cast magnesium was presented in our previous work (Mathis,2004). We showed by means of X-ray diffraction peak profile analysis, that during the tensile test the ***c + a*** slip becomes dominant deformation mechanism above 200°C, whereas the basal slip loses its importance.

Besides the slip in the second order pyramidal slip system, which is obviously a very difficult slip direction, twinning is the only active deformation mode that can provide straining along the *c*–axis at room temperature (Agnew&Duygulu,2005). Generally, those hcp metals that exhibit substantial twinning (e.g. Ti and Zr) possess higher ductility (Yoo,1981). The $\{10\bar{1}2\}\langle 10\bar{1}1\rangle$ twinning mode has been found as the most significant one in magnesium alloys (Barnett,2007). This twinning mode can accommodate extensions along the *c*-axis of the hexagonal lattice but not contractions along the same direction. In tension those grains undergo $\{10\bar{1}2\}$ twinning whose *c*-axis is nearly parallel to the loading direction (Fig. 3). On the contrary, in compression the *c*-axis must be perpendicular to the loading direction for easy activation of $\{10\bar{1}2\}\langle 10\bar{1}1\rangle$ twinning mode (Gharghouri,1999).

In case, when compression acts along the *c*-axis, complex double-twinned structures have been observed, where the twins in the $\{10\bar{1}1\}$ or $\{10\bar{1}3\}$ planes play the key role (Yoshinaga,1973).

Twinning of magnesium alloys is significantly dependent on the microstructural parameters, as e.g. grain size, initial texture and alloying content. The burst character of the AE response due to the twin nucleation enables the *in-situ* monitoring of twinning during the deformation tests. The advantage of the AE method stands upon monitoring the entire sample volume in real time, whereas in e.g. electron microscopy or electron backscattered diffraction , only a small volume of the specimen is investigated in *post-mortem* state.

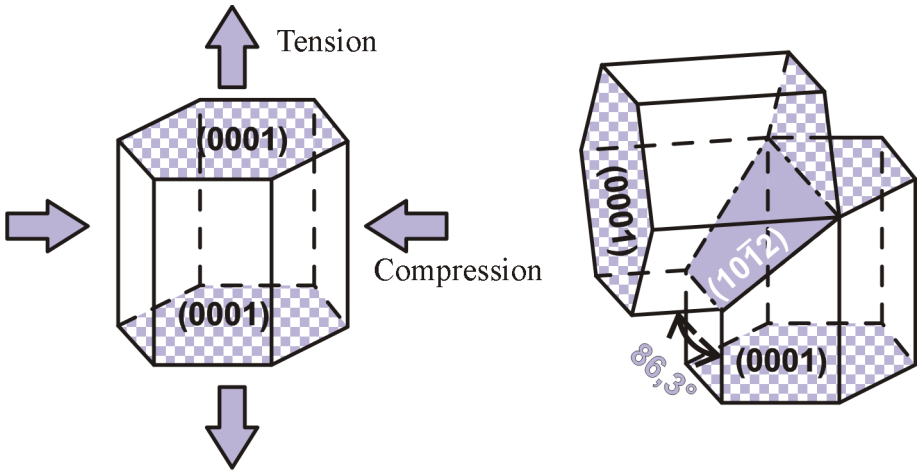

Fig. 3. Scheme of the twinning mechanism with respect to the loading direction.

5.1 Grain size dependence of acoustic emission in polycrystalline magnesium

The effect of grain size on the twinning activity or rather the AE response was studied in texture-free polycrystalline magnesium with 0.04 wt%, 0.15 wt% and 0.35 wt% Zr. (further referred to as Mg04, Mg15 and Mg35, respectively). As a consequence of the different Zr content, the specimens had different grain sizes: 550 μm (Mg04), 360 μm (Mg15) and 170 μm (Mg35). Tensile testing was carried out using specimens with a rectangular cross-section of 5 x 5 mm^2 and a gauge length of 25 mm. Compression testing was performed using prism samples 25 mm long and 15 x 15 mm^2 in cross-section. Tensile specimens were tested to fracture, while in the compression tests the specimens were deformed either to fracture or the tests was stopped after achieving of 20% strain in order to avoid the destruction of the AE sensor. All tests were performed at room temperature and at an initial strain rate of 10^{-3} s^{-1}. The specimens were tested in as-cast condition. AE was monitored directly using a computer-controlled DAKEL-XEDO-3 device. The facility incorporated a high temperature S9215 transducer (Physical Acoustic Corporation) with a flat response between 50 and 650 kHz and a preamplifier giving a gain of ~30 dB. Total gain was about 94 dB. As described earlier, the AE analyzer detects the AE signals at two settable threshold levels, which corresponded to voltages of 730 mV for the total AE count 1 and 1450 mV for the burst AE count 2 (total range of the A/D converter is 2400 mV). The first level was used for the detection of the total AE signal (count rate 1). By setting the second level, we recorded only strong signals caused largely by twins (count rate 2).

The initial microstructure of all investigated specimens exhibited a nearly equiaxed grain structure. The tensile and compression true stress-true strain curves as a function of grain size are shown in Fig. 4. As expected, both yield stress and strength increase with decreasing grain size.

Fig. 5 shows the grain size dependence of the count rate 1 in compression. The largest AE response was observed for the Mg04 sample because of the larger grain size. As it was discussed before, the most important deformation mechanisms in magnesium at room

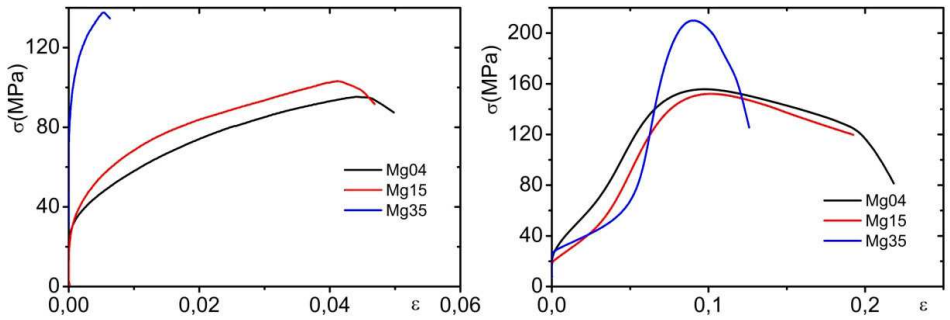

Fig. 4. Grain size dependence of true stress-true strain curves in a) tension; b) compression

temperature are slip of basal dislocations and twinning in system $\{10\bar{1}2\}\langle 10\bar{1}1\rangle$. These mechanisms were identified by Friesel and Carpenter (Friesel&Carpenter,1984) as the main sources of AE during plastic deformation of magnesium polycrystals. The size of grains, their mutual orientation and the structure of grain boundaries are very important for mechanical properties. The plastic deformation is influenced by dislocation pile-ups at the grain boundaries. The grain size dependence of the AE activity is not monotonic, as it is indicated by the numerous experimental data (Heiple&Carpenter,1987a). The largest AE activity was observed in single crystals and the large grained ($d \geq 10^3$ μm) materials, respectively. These observations could be explained in terms of large mean free path of long dislocation lines. In case of smaller grain sizes the AE is influenced by several mechanisms. The larger number of grain boundaries decreases the mean free path of dislocations. Thus the detectable AE activity decreases. On the other hand the number of dislocation sources in the grain boundaries increases (Kishi&Kuribayashi,1977). The velocity of moving dislocation could also increase due to the higher acting stress on dislocations. Nevertheless, the latter two mechanisms are negligible in the grain size range of several hundreds μm (James&Carpenter,1971, Kiesewetter&Schiller,1976) and the AE activity similarly increases with increasing grain size as it can be seen in Fig. 5.

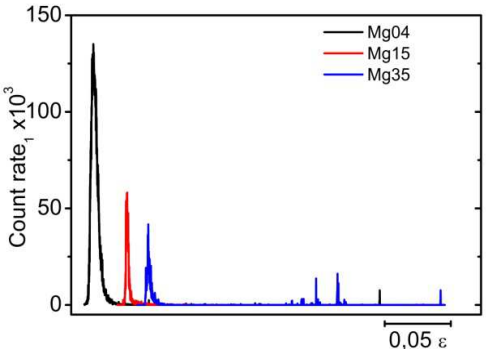

Fig. 5. Grain size dependence of Count rate 1 in compression. Due to better visibility, the curves are shifted along the *x*-axis.

Kim and Kishi (Kim&Kishi,1979) investigated pure aluminum with different grain sizes in range from 26 to 156 μm. They described relation between the RMS voltage and the grain size as:

$$U_{RMS}^2 = B \exp\left(Cd^{-1}\right), \tag{8}$$

where *B* and *C* are constants. Our data set it not sufficient to get good statistics, nevertheless the peak values of the count rate 1 follow an exponential curve (c.f. Fig. 5). The grain size dependence of twinning could be monitored at the second threshold level. The peak areas of the count rate 1 and the count rate 2 for Mg04 and Mg35 are depicted in Fig. 6. It can be seen that for Mg04 approximately 60% of the events crossing the first threshold cross the second threshold as well. On the other hand this fraction for Mg35 specimen is significantly smaller (~20%). It indicated a higher twinning activity and larger twin volume in coarse grained specimen. This result is in accordance with the EBSD observation of Beyerlein et al. (Beyerlein,2010), who found that the number of twins per grain and the twinned fraction increase with grain area.

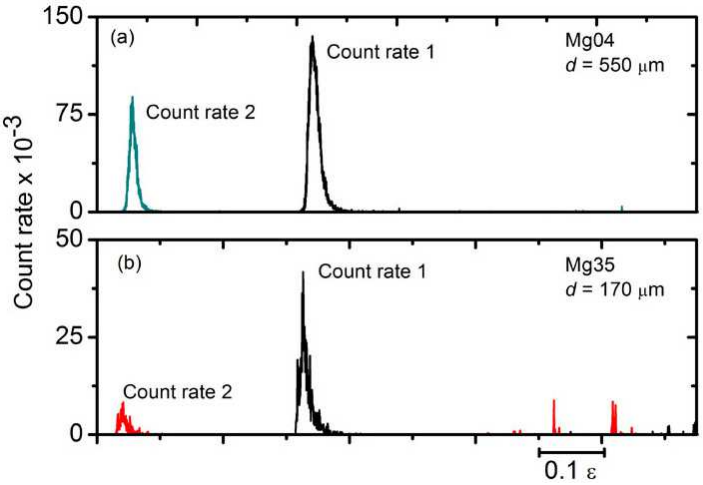

Fig. 6. Comparison of the count rate 1 and the count rate 2 for a) Mg04; b) Mg35 specimens. Due to better visibility, the curves are shifted along the *x*-axis.

5.2 Influence of loading mode and initial texture on the acoustic emission response in various magnesium alloys

As it is evident from Fig. 4, the shape of deformation curves depends on the loading mode. In compression S-shaped curves are observed, i.e. after a low stress plateau a significant hardening takes place. On the other hand, the tension curves are convex and the yield stress is markedly higher than that for the compressed samples (e.g. for Mg04: 58 MPa in tension and 32 MPa in compression). A similar behaviour, called tension-compression asymmetry, has been observed by several authors (Barnett,2007, Jain&Agnew,2007) and is connected with mechanical twinning (Barnett,2007). The comparison of the AE response for tension and compression depicted in Fig. 7 for Mg35 specimen revealed a different evolution of twinning.

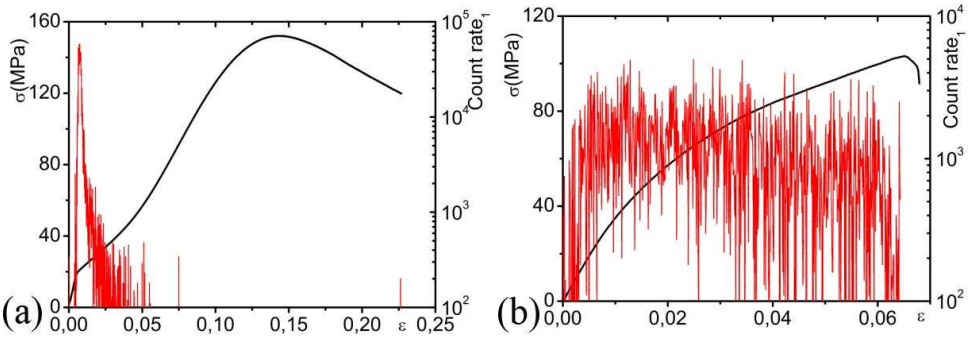

Fig. 7. Dependence of acoustic emission signal on loading mode (a) – compression, (b) – tension).

The signal recorded *in compression* (Fig. 7a) reached its maximum at approx. 1% strain in the low stress plateau range. Similar twinning evolution has been observed in compressed cast magnesium by Klimanek and Pötzsch (Klimanek&Pötzsch,2002). Using light microscopy they found a maximum in the apparent mean volume fraction of the twins in the strain range of 0.05 – 0.1ε. The rapid decrease of the AE signal after reaching the peak indicates the growth of the already present twins rather than nucleation of new twins. Actually, in compression, fast growth of $\{10\bar{1}2\}$ twins was observed (Knezevic,2010). The AE method is sensitive only to twin nucleation, not to twin growth (Friesel&Carpenter,1984), consequently the AE signal decreased. In further course of deformation the non-basal slip systems are activated (Agnew&Duygulu,2005, Clausen,2008). This mechanism increases the dislocation density considerably and thereby it reduces the mean free path of moving dislocations. Since the latter parameter is directly proportional to the AE intensity, the AE signal decreased under the detectable limit. During *tensile straining* burst AE signals were observed. After reaching the maximum, the signal level decreases gradually (Fig. 7b). This behaviour indicates that twin nucleation took place during the entire test. In tension, the nucleation of twins requires higher stresses and their growth is limited (Koike,2005). Our recent work (Máthis,2011), reporting on concurrent measurements of AE and neutron diffraction in deformed Mg - 1 wt.% Zr. supports these assumptions. We found a strong increase in the value of the integrated intensity of twin planes in the vicinity of the yield point. The neutron diffraction method is also capable of monitoring the twin growth. Using this feature we found that despite of different evolution of twinning, the total volume twinned during the tensile and compression deformation does not differ within the experimental error.

The effect of initial texture on the mechanical properties and the AE response could be demonstrated on a rolled sheet from magnesium alloy AZ31 (3 wt.% Al, 1 wt.% Zn, balance Mg). The samples used in this study had a gauge length of 25 mm and 5 x 1.6 mm^2 in cross section. The samples were in H24 temper condition (strain hardened and stress relieved state). The samples exhibited a basal texture with a significant concentration of basal planes oriented into normal direction. Tensile tests were carried out parallel (RD), perpendicular (TD) and under 45° to the rolling direction at a constant strain rate of 4×10^{-4} s^{-1} and at room temperature. Fig. 8a shows the development of engineering stress and the corresponding

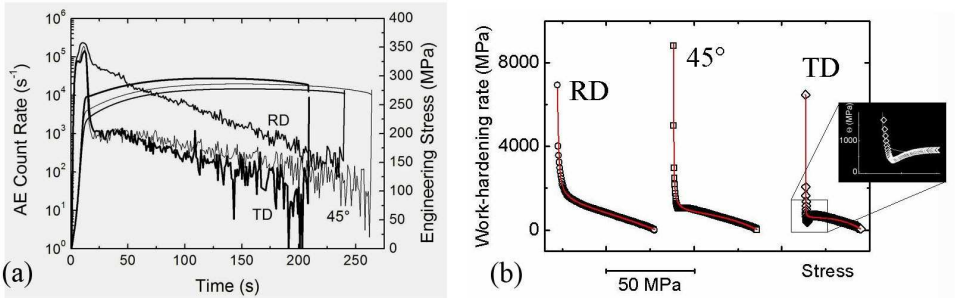

Fig. 8. (a) Development of engineering stress and AE count rate 1 with time, as a function of sample orientation; (b) Work hardening curves corresponding to the deformation curves in the adjacent figure.

AE count rate 1 with time. It is seen that the strength increases towards the TD direction. The course of AE curves exhibits a characteristic maximum related to the macroscopic yield point, which is followed by a decrease. The count rate differs with respect to the direction of the measurement. The decrease of the count rate is faster for TD and 45° specimens. The difference in the mechanical properties among the specimens could be explained in terms of different activation of deformation mechanisms during the testing. In RD, the slip of basal ***a*** dislocations is the dominant mechanism. Since this mechanism does not fulfil the von Mises criterion for plastic deformation, $\{10\bar{1}2\}$ twinning has also to take place (Bohlen,2004). As it has been shown by Yoo (Yoo,1981), the twin boundary is impenetrable for basal dislocations. Thus twinning decreases spacing between the obstacles of non-dislocation type and the AE signal decreases. In later stages of deformation non-basal slip systems (prismatic and/or pyramidal) are activated (Agnew,2003). The orientation relations in TD and 45° samples do not favour the basal slip. Thus, besides twinning, slip in prismatic and pyramidal planes is initiated at the onset of plastic deformation (Agnew,2003, Bohlen,2004). The evidence of non-basal slip is seen from the work hardening curves (Fig. 8b), where a characteristic lift appears in the vicinity of the yield point. Only the pyramidal ***c + a*** dislocations could cross the twin boundaries (Yoo,1981). If the glide ***c + a*** dislocations interact with ***a*** dislocations in the basal plane, immobile ***c*** dislocations may be produced in the basal plane according to the following reaction (Lukac,1985):

$$\tfrac{1}{3}\langle 2\bar{1}\bar{1}3\rangle + \tfrac{1}{3}\langle \bar{2}110\rangle \rightarrow \langle 0001\rangle , \tag{9}$$

Another reaction may yield a sessile ***c + a*** dislocation.

$$\tfrac{1}{3}\langle 2\bar{1}\bar{1}3\rangle + \tfrac{1}{3}\langle \bar{1}2\bar{1}0\rangle \rightarrow \tfrac{1}{3}\langle 11\bar{2}3\rangle , \tag{10}$$

A combination of two glide ***c + a*** dislocations gives rise to a sessile dislocation of ***a*** type that lies along the intersection of the second-order pyramidal planes according to the following reaction:

$$\tfrac{1}{3}\langle 2\bar{1}\bar{1}3\rangle + \tfrac{1}{3}\langle \bar{1}2\bar{1}3\rangle \rightarrow \tfrac{1}{3}\langle 11\bar{2}0\rangle , \tag{11}$$

Production of sessile dislocations increases the density of the forest dislocations that are obstacles for moving dislocations. Thus, the increase in the flow stress with straining is caused by increasing amount of obstacles. Furthermore, reduced mean free path of dislocation causes a rapid drop of the AE signal activity.

5.3 Dependence of acoustic emission on the testing temperature in polycrystalline magnesium

The influence of testing temperature on the AE response was studied on the alloy AZ31 prepared by continuous casting (Vidrich,2008). The compression tests were performed in the temperature range from 20°C to 300°C at an initial strain rate of 10^{-3} s^{-1}. The specimen size and the AE transducer were the same, as in experiments described in the section 5.1. The AE transducer was fixed directly on the sample. The AE count rate curves as a function of temperature for samples with a grain size of 150 μm showed a distinct maximum at 200°C (c.f. Fig. 9). The strong temperature dependence of AE was likely caused by the influence of thermally-activated processes. We believe that it was the activity of non-basal slip systems. It has been shown recently by Chapuis and Driver (Chapuis&Driver,2011), that the CRSS for $\{10\bar{1}2\}$ twinning and pyramidal slip decreases with increasing testing temperature. The maximum count rate, observed at 200°C, may have been a result of the synergistic effect of both mechanisms. Twinning activity probably reached its maximum at this point. Pyramidal slip systems are also active at this temperature, as we showed by X-ray methods (Mathis,2004). Decreasing AE activity above this temperature is influenced by both recrystallization and the activity of non-basal slip systems (Chapuis&Driver,2011, Mathis,2004). Since at 300°C the CRSS for pyramidal slip system is lower than that for twinning (Yoshinaga&Horiuchi,1964), its activation is more favorable than twinning. The decrease of number of twins at 300°C in pure magnesium and AZ31 magnesium alloy was observed also by Sitdikov (Sitdikov,2003) and Myshlyaev (Myshlyaev,2002). Nevertheless, the twinning does not disappear completely – the AE activity still involves strong bursts. Myshlyaev (Myshlyaev,2002) assumed that at high temperature dislocations in twin boundaries quickly annihilate. Furthermore the twins could interact with non-basal dislocations and decompose. This mechanism could alter the mutual orientation of the twin and the matrix. Dislocations piled-up at new matrix-twin boundaries

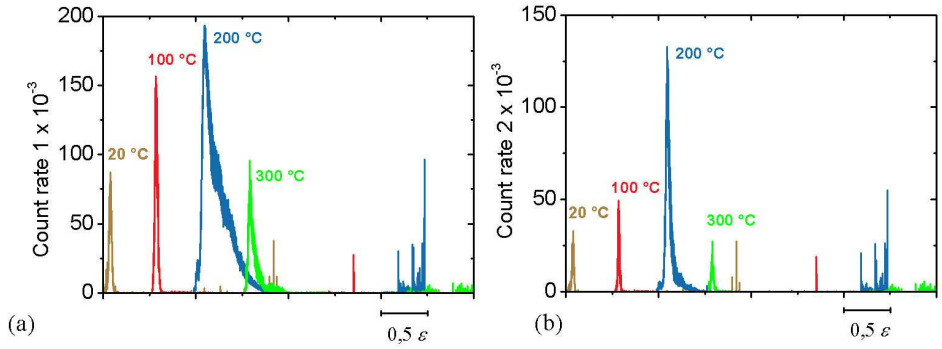

Fig. 9. Temperature dependence of the count rates 1 and 2 for the AZ31 alloy (compression test)

cause a stress field that could lead to activation of additional non-basal dislocations. Screw components of ***c + a*** (and also ***a***) dislocations may move to the parallel slip planes by double cross slip and annihilate, which decreases dislocation density and results in softening. Due to the lower twinning activity and the non-collective character of the softening, a strong decrease in the AE count rate was observed.

5.4 Acoustic emission from magnesium-based composites

Magnesium-based MMCs have been developed and manufactured over the last two decades for potential use as lightweight high-performance materials especially in the transportation industry. The standard operating conditions for most MMCs involve thermal and/or mechanical loading. This may induce microstructural changes and matrix plastic deformation characterized by dislocation generation and motion. In addition, for the case of MMCs thermal loading induces internal stresses owing to the often substantial mismatch between the thermal expansion coefficients of the matrix and the reinforcement. Under higher load and/or long-term exposure, structural damage (for example, interface de-cohesion, fiber fracture) may also occur. The main advantage of monitoring AE during either processing or straining of MMCs is in revealing the structural damages earlier than with other non-destructive methods (Miller&Hill,2005). However, there are only limited results demonstrating the use of AE in investigation of magnesium-based MMCs.

The matrix material used in this investigation was Mg of commercial purity. The matrix was reinforced with 20 vol. % of Saffil® δ-Al_2O_3 short fibers through the squeeze-casting procedure in which the molten Mg is infiltrated under pressure into short fiber pre-forms. The fabricated MMCs showed a planar isotropic fiber distribution (fiber diameters of ~3-5 μm and fiber lengths up to ~150 μm). There was a slight chemical reaction between the matrix and the reinforcement which led to chemical bonding at the interfaces. In addition, the matrix in the vicinity of the interfaces became enriched in aluminum. Specimens were machined for thermal cycling in the form of rods with lengths of 50 mm and diameters of 5 mm: the reinforcement planes in these samples were parallel to the longitudinal axes. Thermal cycling was conducted *in-situ* by placing the specimens within a dilatometer equipped with a radiant furnace permitting temperatures from ambient up to 400ºC. The residual strain was measured after each cycle and the AE signal was transmitted through a quartz rod in contact with the specimen.

Figure 10a shows the variation with time of the AE count rate 1, $\dot{N}_{C1}$, and the specimen deformation, Δl, with the temperature, T, during a single temperature cycle having upper temperatures, T_{top}, of 300°C and 400°C, respectively. It is apparent that there is moderate AE during the heating within a temperature range from ~140°C to ~220°C and significant AE during the cooling of the sample at temperatures from ~180°C to room temperature. Following the cycles, a residual contraction was measured in the samples. The behaviour of the composite during thermal cycling was characterised in detail by using a stepped incremental temperature technique. The results are documented in Fig. 10b where the residual strain, $\Delta l/l_o$, and the AE count per cycle, N_{C1} are plotted against the upper cycle temperature, T_{top}, where l_o is the original length of the sample and one cycle was performed for each upper temperature corresponding to each separate experimental point recorded for the residual strain. This plot demonstrates that there is no residual strain up to a certain upper temperature, followed by a

slight tendency for a compressive contraction. The residual elongation prevails in a certain temperature interval and for higher upper temperatures there is a residual contraction that increases in magnitude with increasing values of T_{top}. The AE response also depends on the upper temperature, increasing significantly at a critical value of T_{top} and exhibiting intense AE bursts which appear with a further increase in T_{top}.

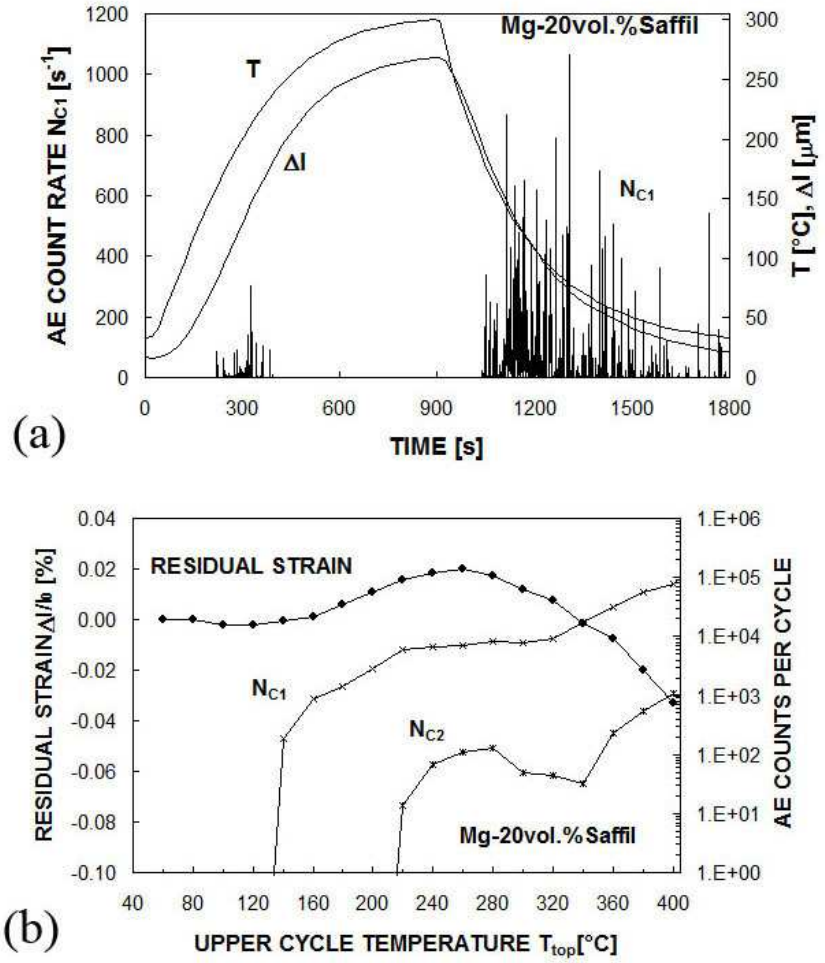

Fig. 10. (a) Value of the AE count rate 1, temperature and sample deformation (Δl) during temperature cycles to upper temperature of 300°C. (b) Residual strain, $\Delta l / l_0$, and AE counts for two different detection levels, N_{C1} and N_{C2}, versus the upper cycling temperature, T_{top}: the residual strain was estimated with reference to a temperature of 30°C and the AE counts were evaluated for the entire cooling period of each cycle.

It has been shown that, under conditions similar to those used in these experiments, more than 1000 thermal cycles are needed in order to produce any measurable damage in the samples (Kiehn,1994). Thus, the AE counts recorded in these experiments must be attributed to the occurrence of structural changes in the matrix and to any associated plastic deformation. Since the MMCs were fabricated by squeeze-casting at an elevated temperature, the composites contain thermal residual stresses at room temperature due to the mismatch in the thermal expansion coefficients between the matrix and the reinforcement (Arsenault&Taya,1987, Xia&Langdon,1994) and the magnitude of these stresses is of the order of the minimum stress required for creep in the matrix. In practice, the matrix in these MMCs experiences tensile stresses whereas the fiber reinforcements experience compressive stresses. Therefore, when the MMC is heated, the internal tensile stress acting on the matrix reduces to zero and, on further heating, there is a build up of compressive stresses; whereas on cooling, the internal stresses behave in the opposite sense. It is anticipated these stresses will be concentrated near the matrix-fiber interfaces and at the ends of the reinforcing fibers. These thermal stresses may also exceed the matrix yield stress within discrete temperature ranges and relaxation will then occur through the generation of new dislocations and plastic deformation within the matrix. This plastic deformation may appear as dislocation glide, as twinning or possibly as grain boundary sliding at the higher temperatures depending upon the precise temperature and the crystallographic structure of the matrix. In general, it is reasonable to anticipate that the compressive deformation that appears on heating will give some form of diffusion-controlled high temperature creep whereas the tensile deformation appearing on cooling will lead to dislocation glide and twinning. Thus, and in support of the experimental observations, a larger AE is expected during cooling at the lower temperatures.

It was suggested earlier that it may be possible to correlate the AE response and the internal thermal stresses produced during thermal cycling (Chmelik,1997). With respect to the dependence of the residual strain on the upper cycle temperature as plotted in Fig. 10a, a quantitative analysis of internal thermal stresses has been developed for a short-fiber reinforced aluminum composite exhibiting chemical bonding at the interfaces (Urreta,1996) and more recently this approach has been further developed and applied to experimental data (Carreno-Morelli,2000). The analysis predicts that the thermal stresses, σ_{TS}, produced by a temperature change at the interfaces of ΔT are given by

$$\sigma_{TS} = \frac{E_f E_M}{E_f f + E_M (1-f)} f \Delta\alpha \, \Delta T \,, \tag{12}$$

where E_f and E_M are the values of Young's modulus for the reinforcement and the matrix, respectively, f is the volume fraction of fibres and $\Delta\alpha$ is the difference between thermal expansion coefficients of the matrix and the reinforcement between the matrix and the reinforcement associated with the coefficients of thermal expansion.

For the composite used in these experiments, E_f = 300 GPa and E_M = 45 GPa at room temperature, f = 0.20, $\Delta\alpha = 20 \times 10^{-6}$ K^{-1} and the decrease in E_M with increasing temperature is ~50 MPa K^{-1}. Thus, Eq. 12 predicts that a temperature change by 1°C produces an increment in the thermal stress of ~0.6 MPa and at temperatures above ~250°C this increment decreases to ~0.4 MPa K^{-1}.

It is shown in Figure 10b that slight but measurable compressive deformation occurs in Mg-Saffil during cycling at upper temperatures above ~100°C and tensile deformation appears during cycling at upper temperatures above ~140°C. It follows from Eq. 12 that a temperature change of 70°C produces a thermal stress of ~40 MPa and, by comparison with the reported compressive acoustic yield (micro-yield) stress of ~20 MPa for the squeeze-cast unreinforced Mg at 100°C (Szaraz&Trojanova,2011), this implies the presence of an initial internal tensile stress of ~20 MPa. A similar calculation may be performed for cooling of the sample from ~140°C since, on heating, a temperature change of 110°C produces a thermal stress of ~60 MPa so that the matrix experiences a compressive stress of ~40 MPa at 140°C. This stress exceeds the matrix yield stress at this temperature and is relaxed by matrix plastic deformation (cf. observed AE) to values below ~15 – 20 MPa. Cooling of the composite to room temperature produces an estimated thermal stress of ~70 MPa. Consequently, a tensile stress approaching ~40 MPa should appear at temperatures near to room temperature and this will correspond to the macroscopic yield point. This effect will lead to AE, as observed experimentally. It is noteworthy that the disappearance of AE during heating at 220°C indicates a change in the deformation mechanism towards high temperature creep. Further details about the AE response of Mg-based MMCs during tensile test could be found in works of Trojanová et al. (Trojanova,2010, Trojanova,2011).

6. Continuous signal sampling - new approach in the acoustic emission measurement

Thanks to the fast developments in computing technology, a qualitatively new approach to the AE measurements can be proposed. Continuous sampling and storage of AE signal (called *data streaming* in Physical Acoustic Corp. terminology) offer a possibility of post-processing of the raw signal. The advantage of this approach is that the results are not influenced by setting up experimental parameters, e.g. threshold, dead-time etc. During the post-processing it is possible to run various successive analyses, evaluate individual time moments with respect to the properties of the whole data set and perform time consuming analyses that would not be possible in real time, i.e. during the experiment. To our knowledge, there are two AE systems on the market offering this feature: (1) New generation DAKEL-CONTI-4 AE system allows continuous sampling and storage of AE signal from 1 up to 4 channels with 2 MHz sampling frequency. The sampled AE signal is continuously stored on a dedicated hard disk connected to the measuring unit via a high speed interface, i.e. no data processing by the computer used to control the measuring unit takes place and a high data transfer speed is ensured. The software enables both the evaluation of individual AE events in a standard way and the analysis of the complete data set based on statistical method (Kral,2007). (2) The on-board PCI-2, 2-channel data acquisition and digital signal processing AE system is manufactured by Physical Acoustic Corporation. The system proceeds with real time AE waveform and signal processing features. The AE Data Streaming function allows continuous recording of AE waveforms to the hard disk at up to 10 MSamples/s rate. The system includes 2 parametric inputs for recording external experimental parameters (e.g. load, extension).

The method offers e.g. a new experimental insight regarding the intermittency character of plastic deformation (crackling plasticity). It was observed that the collective dislocation dynamics self-organizes into a scale-free pattern of dislocation avalanches characterized by

intermittency, power law distributions of avalanche sizes (Groma,2003), aftershock triggering (Weiss&Miguel,2004) as well as fractal patterns (Weiss&Miguel,2004). This crackling noise (Bailey,2000) suggests reconsidering dislocation-driven plasticity within a close-to-criticality non-equilibrium framework. These observations are supported by discrete dislocation dynamics (Groma,2003), continuum (Zaiser,2006) and phase-field (Koslowski,2004) numerical models, which indicate that the observed picture might be of generic nature in plastic deformation of crystalline materials. Direct observation of dislocation avalanches in real time is rather difficult, usually micron-size samples are necessary (Ispanovity,2010). We have shown in our previous work (Richeton,2007) on Cd and Zn-0.08 wt.%Al single crystals that the above described effects could be monitored through continuous AE signal sampling. All stages of plastic deformation in both hcp-structured specimens were characterized by a strong intermittent AE activity (Fig. 11a). The AE signals recorded during stage I (easy basal glide) where twinning is absent, indicate the occurrence of dislocation glide avalanches, as it was observed previously in ice (Richeton,2005). The relative proportion of twinning events vs. slip avalanches increased from stage I to stage III, as expected. Whatever the material or the stage of deformation, a power law distribution of probability density of AE energy was observed, i.e. $P(E) \sim E^{-\tau_E}$, with the exponent $\tau_E = 1.6 \pm 0.1$ (Fig. 11b). This demonstrates that the generic character of crackling plasticity is not restricted to single-slip systems (such as ice), but is also observed in the presence of forest hardening or twinning. Twinning and slip avalanches can be discriminated from the AE waveforms and both populations are characterized by the same power law distribution (Richeton,2006). Plastic instabilities are clustered in time, as manifested by the presence of aftershocks. Moreover, it was shown that twinning events can trigger slip avalanches, or the reverse, suggesting that both types of instabilities participate to the same global critical-like dynamics.

The intrinsic structure of AE events during jerky flow in an aluminium alloy was also examined by this method with success (Weiss,2007).

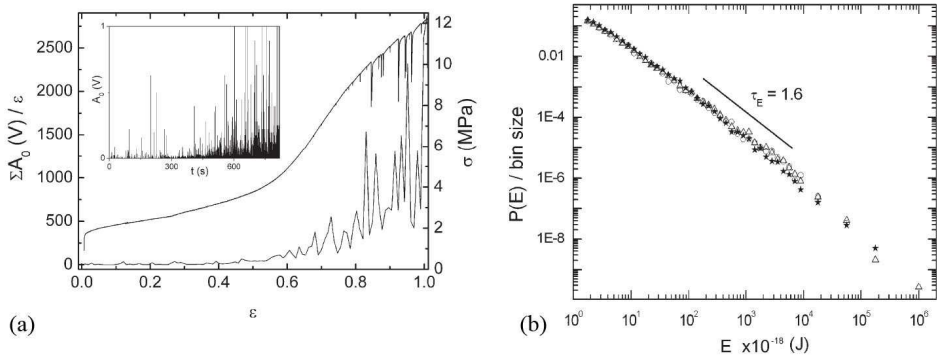

Fig. 11. (a) The stress-strain curve and the evolution of the AE activity during deformation of the sample Zn-0.08 wt.%Al. The curve represents the amplitudes of the AE events (A_0) cumulated over a time window of 7 s and normalized by the corresponding strain. The inset shows the recorded AE signal. (b) Distribution of AE energies recorded during the plastic deformation of hcp metallic single crystals. Triangles: Cd, strong forest hardening + twinning. Circles: Cd, stage I, easy basal glide. Stars: Zn-0.08wt.%Al. In courtesy of Dr. Patrik Dobroň.

7. Conclusions

In this chapter the potential of the AE technique as *in-situ* tool for monitoring of plastic deformation processes of hexagonal closed packed materials was presented. It was shown that both deformation twinning and dislocation glide are the major sources of AE. The capability of the AE measurements for investigating of magnesium-based metal matrix composites and of the intermittency character of plastic deformation was also discussed.

8. Acknowledgment

This work is part of the research program of MSM 0021620834 financed by the Ministry of Education, Youth and Sports of the Czech Republic. The authors are grateful for the financial support of the Czech Science Foundation under the contract P108/11/1267. Assistance of our students Zuzana Zdražilová and Jan Čapek from Charles University during experiments is also acknowledged.

9. References

Agarwal, A. B. L., Frederic, J. R. and Felbeck, D. K. (1970). Detection of plastic microstrain in aluminum by acoustic emission. *Met. Trans.*, Vol.1, No.4, pp. (1069-1071), 0026-086X

Agnew, S. R. and Duygulu, O. (2005). Plastic anisotropy and the role of non-basal slip in magnesium alloy AZ31B. *International Journal of Plasticity*, Vol.21, No.6, pp. (1161-1193), 0749-6419

Agnew, S. R., Tome, C. N., Brown, D. W., Holden, T. M. and Vogel, S. C. (2003). Study of slip mechanisms in a magnesium alloy by neutron diffraction and modeling. *Sci. Mat.*, Vol.48, No.8, (Apr), pp. (1003-1008), 1359-6462

Agnew, S. R., Yoo, M. H. and Tome, C. N. (2001). Application of texture simulation to understanding mechanical behavior of Mg and solid solution alloys containing Li or Y. *Acta Mater.*, Vol.49, No.20, (Dec), pp. (4277-4289), 1359-6454

Ando, S. and Tonda, H. (2000). Non-basal slip in magnesium-lithium alloy single crystals. *Materials Transactions Jim*, Vol.41, No.9, (Sep), pp. (1188-1191), 0916-1821

Arsenault, R. J. and Taya, M. (1987). Thermal-resiudual stress in metal matrix composite. *Acta Metall.*, Vol.35, No.3, (Mar), pp. (651-659), 0001-6160

Avedesian, M. M. and Baker, H. *Magnesium and Magnesium Alloys (ASM Specialty Handbook)* ASM International, 0-87170-657-1,

Bailey, N. P., Sethna, J. P. and Myers, C. R. (2000). Dislocation mobility in two-dimensional Lennard-Jones material In: *Multiscale Phenomena in Materials-Experiments and Modeling,* I. M. Robertson, D. H. Lassila, B. Devincre and R. Phillips, pp. (249-254), Materials Research Society Symposium Proceedings, 0272-9172,

Barnett, M. R. (2007). Twinning and the ductility of magnesium alloys Part I: "Tension" twins. *Mater. Sci. Eng. A*, Vol.464, No.1-2, (Aug), pp. (1-7), 0921-5093

Beyerlein, I. J., Capolungo, L., Marshall, P. E., McCabe, R. J. and Tome, C. N. (2010). Statistical analyses of deformation twinning in magnesium. *Phil. Mag.*, Vol.90, No.16, pp. (2161-2190), 1478-6435

Blish, R. C. and Vreeland, T. (1969). Dislocation velocity (1-2-12) 12-13 slip systems of zinc. *Journal of Applied Physics*, Vol.40, No.2, pp. (884-890), 0021-8979

Bohlen, J., Chmelik, F., Dobron, P., Kaiser, F., Letzig, D., Lukac, P. and Kainer, K. U. (2004). Orientation effects on acoustic emission during tensile deformation of hot rolled magnesium alloy AZ31. *J. Alloy. Compd.*, Vol.378, No.1-2, (Sep), pp. (207-213), 0925-8388

Carpenter, S. H. and Chen, C. M. (1988). The Acoustic Emission Generated during the Plastic Deformation of High Purity Zinc. *J. Acoust. Em.*, Vol.7, No.4, pp. (161-166), 0730-0050

Carreno-Morelli, E., Urreta, S. E. and Schaller, R. (2000). Mechanical spectroscopy of thermal stress relaxation at metal-ceramic interfaces in aluminum-based composites. *Acta Mater.*, Vol.48, No.18-19, (Dec), pp. (4725-4733), 1359-6454

Chapuis, A. and Driver, J. H. (2011). Temperature dependency of slip and twinning in plane strain compressed magensium single crystals. *Acta Mater.*, Vol.59, pp. (1986-1994),

Chmelik, F., Kiehn, J., Lukac, P., Kainer, K. U. and Mordike, B. L. (1997). Acoustic emission and dilatometry for non-destructive characterisation of microstructural changes in Mg based metal matrix composites submitted to thermal cycling. *Scripta Mat.*, Vol.38, No.1, (Dec), pp. (81-87), 1359-6462

Clausen, B., Tome, C. N., Brown, D. W. and Agnew, S. R. (2008). Reorientation and stress relaxation due to twinning: Modeling and experimental characterization for Mg. *Acta Mater.*, Vol.56, No.11, (Jun), pp. (2456-2468), 1359-6454

Czochralski, J. (1916). Metallographie des Zinns und die Theorie der Formänderung bildsamer Metalle. *Metall und Erz*, Vol.22, pp. (381-393), 1011-4602

Dunegan, H. L. (1963). *Acoustic Emission: A Promising Technique,* UCID-4643, Lawrence Radiation Laboratory, Livermore, CA.

Eshelby, J. D. (1962). Interaction of Kinks and Elastic Waves. *Proceedings of the Royal Society of London Series a-Mathematical and Physical Sciences*, Vol.266, No.1325, pp. (222-246),

Friesel, M. and Carpenter, S. H. (1984). Determination of the Source of Acoustic Emission Generated during the Deformation of Magnesium. *J. Acoust. Em.*, Vol.6, pp. (11-18),

Gharghouri, M. A., Weatherly, G. C., Embury, J. D. and Root, J. (1999). Study of the mechanical properties of Mg-7.7at.% Al by in-situ neutron diffraction. *Philosophical Magazine a-Physics of Condensed Matter Structure Defects and Mechanical Properties*, Vol.79, No.7, (Jul), pp. (1671-1695), 0141-8610

Gillis, P. P. and Hamstad, M. A. (1974). Some fundamental aspects of theory of acoustic-emission. *Mater. Sci. Eng. A*, Vol.14, No.2, pp. (103-108), 0025-5416

Granato, A. and Lücke, K. (1956). Theory of mechanical damping due to dislocations. *Journal of Applied Physics*, Vol.27, No.6, pp. (583-593), 0021-8979

Groma, I., Csikor, F. F. and Zaiser, M. (2003). Spatial correlations and higher-order gradient terms in a continuum description of dislocation dynamics. *Acta Mater.*, Vol.51, No.5, (Mar), pp. (1271-1281), 1359-6454

Hatano, H. (1975). Quantitative measurements of acoustic emission related to its microscopic mechanisms *Journal of Acoustic Society of America*, Vol.57, No.3, pp. (639-645), 0001-4966

Heiple, C. R. and Adams, R. O. (1976) Acoustic Emission from Beryllium *Proceedings of Third Acoustic Emission Symposium*, Tokyo,

Heiple, C. R. and Carpenter, S. H. (1987a). Acoustic Emission Produced by Deformation of Metals and Alloys - A Review: Part I. *J. Acoust. Em.*, Vol.6, No.2, pp. (177-204),

Heiple, C. R. and Carpenter, S. H. (1987b). Acoustic Emission Produced by Deformation of Metals and Alloys - A Review: Part II. *J. Acoust. Em.*, Vol.6, No.4, pp. (215-237),

Higgins, F. P. and Carpenter, S. H. (1979). Damping in iron during and after deformation. *Mater. Sci. Eng. A*, Vol.37, No.2, pp. (173-178), 0025-5416

Hirth, J. P. and Lothe, J. *Theory of dislocations* John Wiley & Sons, 0-471-09125-1, New York

Hutchinson, J. W. (1977). Creep and plasticity of hexagonal polycrystals as related to single-crystal slip. *Metall. Trans. A*, Vol.8, No.9, pp. (1465-1469), 0360-2133

Ispanovity, P. D., Groma, I., Gyorgyi, G., Csikor, F. F. and Weygand, D. (2010). Submicron Plasticity: Yield Stress, Dislocation Avalanches, and Velocity Distribution. *Phys. Rev. Lett.*, Vol.105, No.8, (Aug), pp. 0031-9007

Jain, A. and Agnew, S. R. (2007). Modeling the temperature dependent effect of twinning on the behavior of magnesium alloy AZ31B sheet. *Mater. Sci. Eng. A*, Vol.462, No.1-2, (Jul), pp. (29-36), 0921-5093

James, D. R. and Carpenter, S. H. (1971). Relationship between acoustic emission and dislocation kinetics in crystalline solids. *Journal of Applied Physics*, Vol.42, No.12, pp. (4685-4697), 0021-8979

Joffe, A. F. (June 1928). *The Physics of Crystals* McGraw-Hill, New York

Kaiser, J. (1950). *Untersuchung über das Auftreten von Geräuschen beim Zugversuch,* PhD thesis, Technische Universität München München.

Kiehn, J., Kohler, C. and Kainer, K. U. (1994). Deformation of short-fiber-reinforced Mg alloys caused by thermally-induced stresses In: *Plasticity of Metals and Alloys - Ispma 6,* P. Lukac, pp. (37-41), Key Engineering Materials, Trans Tech Publications, 0252-1059, Clausthal Zellerfeld

Kiesewetter, N. and Schiller, P. (1976). Acoustic-Emission from moving dislocations in aluminum. *Phys. Stat. Sol. a*, Vol.38, No.2, pp. (569-576), 0031-8965

Kim, H. C. and Kishi, T. (1979). Grain-size and flow-stress dependence of acoustic emission energy-release in polycrystalline aluminum. *Phys. Stat. Sol. a*, Vol.55, No.1, pp. (189-195), 0031-8965

Kishi, T. and Kuribayashi, K. (1977). Acoustic emission in the process of plastic deformation and its interpretation. *Kinzoku*, Vol.47, No.7, pp. (67-72),

Klimanek, P. and Pötzsch, A. (2002). Microstructure evolution under compressive plastic deformation of magnesium at different temperatures and strain rates. *Mater. Sci. Eng. A-Struct. Mater. Prop. Microstruct. Process.*, Vol.324, No.1-2, (Feb), pp. (145-150), 0921-5093

Knezevic, M., Levinson, A., Harris, R., Mishra, R. K., Doherty, R. D. and Kalidindi, S. R. (2010). Deformation twinning in AZ31: Influence on strain hardening and texture evolution. *Acta Mater.*, Vol.58, No.19, (Nov), pp. (6230-6242), 1359-6454

Koike, J. (2005). Enhanced deformation mechanisms by anisotropic plasticity in polycrystalline Mg alloys at room temperature. *Metall. Mater. Trans. A*, Vol.36A, No.7, (Jul), pp. (1689-1696), 1073-5623

Kosevich, A. M. (1964). Dinamicheskaya teoriya dislokacii. *Uspekhi Fizicheskikh Nauk*, Vol.84, No.4, pp. (579-609), 0042-1294

Koslowski, M., LeSar, R. and Thomson, R. (2004). Avalanches and scaling in plastic deformation. *Phys. Rev. Lett.*, Vol.93, No.12, (Sep), pp. 0031-9007

Kral, R., Dobron, P., Chmelik, F., Koula, V., Rydlo, M. and Janecek, M. (2007). A qualitatively new approach to acoustic emission measurements and its application to pure aluminium and Mg-Al alloys. *Kov. Mater.-Met. Mater.*, Vol.45, No.3, pp. (159-163), 0023-432X

Lord, A. E. (1981). Acoustic Emission - An Update In: *Physical Acoustic, Principles and Methods,* W. P. Mason and R. N. Thurson, pp. (295-360), Academic Press, 012-477-915-8, New York

Lukac, P. (1985). Hardening and softening during plastic-deformation of hexagonal metals. *Czechoslovak Journal of Physics*, Vol.35, No.3, pp. (275-285), 0011-4626

Máthis, K., Beran, P., Čapek, J. and Lukáš, P. (2011). In-situ neutron diffraction and acoustic emission investigation of twinning activity in magnesium *Journal of Physics-Conference series*, pp. (in press), 1742-659

Mathis, K., Nyilas, K., Axt, A., Dragomir-Cernatescu, I., Ungar, T. and Lukac, P. (2004). The evolution of non-basal dislocations as a function of deformation temperature in pure magnesium determined by X-ray diffraction. *Acta Mater.*, Vol.52, No.10, (Jun 7), pp. (2889-2894), 1359-6454

Miller, R. K. and Hill, E. v. K. *Acoustic Emission Testing* American Society for Nondestructive Testing, 1-57117-106-1, Columbus

Myshlyaev, M. M., McQueen, H. J., Mwembela, A. and Konopleva, E. (2002). Twinning, dynamic recovery and recrystallization in hot worked Mg-Al-Zn alloy. *Mater. Sci. Eng. A*, Vol.337, No.1-2, (Nov), pp. (121-133), 0921-5093

Natsik, V. D. and Burkanov, A. N. (1972). Radiation of Rayleigh Waves by an Edge Dislocation Emerged on Crystal Surface. *Fizika Tverdogo Tela*, Vol.14, No.5, pp. (1289-1296), 0367-3294

Natsik, V. D. and Chishko, K. A. (1972). Sound Radiation during Annihilation of Dislocations. *Fizika Tverdogo Tela*, Vol.14, No.11, pp. (3126-3132), 0367-3294

Natsik, V. D. and Chishko, K. A. (1975). Dynamics and Sound Radiation of Dislocation Frank-Read Source. *Fizika Tverdogo Tela*, Vol.17, No.1, pp. (342-345), 0367-3294

Natsik, V. D. and Chishko, K. A. (1978). Sound Radiation of Dislocations Moving near a Surface of Crystal. *Fizika Tverdogo Tela*, Vol.20, No.2, pp. (457-465), 0367-3294

Obara, T., Yoshinaga, H. and Morozumi, S. (1973). 11-22 (11-23) slip system in magnesium. *Acta Metall.*, Vol.21, No.7, pp. (845-853), 0001-6160

Papirov, I. I., Karpov, E. S., Palatnik, M. I. and Mileshkin, M. B. (1984). Acoustic-Emission during Plastic and Superplastic Deformation of a Zn-0.4-percent Al-Alloy. *Metal Science and Heat Treatment*, Vol.26, No.11-1, pp. (887-891), 0026-0673

Paton, N. E. and Backofen, W. A. (1970). Plastic deformation of titanium at elevated temperatures. *Metall. Trans.*, Vol.1, No.10, pp. (2839-2846), 0026-086X

Richeton, T., Dobron, P., Chmelik, F., Weiss, J. and Louchet, F. (2006). On the critical character of plasticity in metallic single crystals. *Mater. Sci. Eng. A*, Vol.424, No.1-2, (May), pp. (190-195), 0921-5093

Richeton, T., Weiss, J. and Louchet, F. (2005). Dislocation avalanches: Role of temperature, grain size and strain hardening. *Acta Mater.*, Vol.53, No.16, (Sep), pp. (4463-4471), 1359-6454

Richeton, T., Weiss, J., Louchet, F., Dobron, P. and Chmelik, F. (2007). Critical character of plasticity from AE experiments in hcp and fcc metals. *Kov. Mater.-Met. Mater.*, Vol.45, No.3, pp. (149-152), 0023-432X

Scruby, C., Wadley, H. and Sinclair, J. E. (1981). The oirigin of acoustic-emission during deformation of aluminum and an aluminum-magnesium alloy. *Philos. Mag. A*, Vol.44, No.2, pp. (249-274), 0141-8610

Sedgwick, R. T. (1968). Acoustic emission from single crystals of LiF and KC1. *Journal of Applied Physics*, Vol.39, No.3, pp. (1728-1740), 0021-8979

Sitdikov, O., Kaibyshev, R. and Sakai, T. (2003). Dynamic recrystallization based on twinning in coarse-grained Mg In: *Magnesium Alloys 2003, Pts 1 and 2,* Y. Kojima, T. Aizawa, K. Higashi and S. Kamado, pp. (521-526), Materials Science Forum, Trans Tech Publications Ltd, 0255-5476, Zurich-Uetikon

Sklenicka, V. and Langdon, T. G. (2004). Creep properties of a fiber-reinforced magnesium alloy. *Journal of Materials Science*, Vol.39, No.5, (Mar), pp. (1647-1652), 0022-2461

Stephens, R. W. B. and Pollock, A. A. (1971). Waveforms and frequency spectra of acoustic emissions. *Journal of Acoustic Society of America*, Vol.3, No.2, pp. (904-910), 0001-4966

Stohr, J. F. and Poirier, J. P. (1972). Electron-microscope study of pyramidal slip [11-22] [11-23] in magnesium. *Phil. Mag.*, Vol.25, No.6, pp. (1313-1330), 0031-8086

Szaraz, Z. and Trojanova, Z. (2011). Enhanced Plasticity of WE54/SiC Composite Prepared by Powder Metallurgy In: *Materials Structure & Micromechanics of Fracture,* P. Sandera, pp. (419-422), Key Engineering Materials, 1013-9826,

Tatro, C. A. (1957). Sonic technique in the detection of crystal slip in metal. *Engineering Research*, Vol.1, pp. (23-28),

Tetelman, A. S. (1972) Acoustic emission and fracture mechanics *Proceedings of US-Japan Joint Symposium on Acoustic Emission*, Tokyo,

Thompson, N. and Millard, D. J. (1952). Twin formation in cadmium. *Phil. Mag.*, Vol.43, No.339, pp. (422-440), 0031-8086

Trojanova, Z., Szaraz, Z., Chmelik, F. and Lukac, P. (2010). Acoustic emission from deformed Mg-Y-Nd alloy and this alloy reinforced with SiC particles. *J. Alloy. Compd.*, Vol.504, No.2, (Aug), pp. (L28-L30), 0925-8388

Trojanova, Z., Szaraz, Z., Chmelik, F. and Lukac, P. (2011). Acoustic emission from deformed magnesium alloy based composites. *Mater. Sci. Eng. A*, Vol.528, No.6, (Mar), pp. (2479-2483), 0921-5093

Urreta, S. E., Schaller, R., CarrenoMorelli, E. and Gabella, L. (1996). The internal damping of Al-Al2O3(f) composites during thermal cycling: The effect of fibre content and matrix strength. Vol.6, No.C8, (Dec), pp. (747-750), 1155-4339

Vidrich, G. (2008). *Grain refinement and dispersion-strengthening with finest ceramic particles,* PhD thesis, Technical University Clausthal, Clausthal-Zellerfeld.

Vinogradov, A. V., Patlan, V. and Hashimoto, S. (2001). Spectral analysis of acoustic emission during cyclic deformation of copper single crystals. *Phil. Mag. A*, Vol.81, No.6, (Jun), pp. (1427-1446), 0141-8610

von Mises, R. (1928). Mechanics of the ductile form changes of crystals. *Zeitschrift Fur Angewandte Mathematik Und Mechanik*, Vol.8, pp. (161-185), 0044-2267

Weiss, J. and Miguel, M. C. (2004). Dislocation avalanche correlations. *Mater. Sci. Eng. A*, Vol.387, pp. (292-296), 0921-5093

Weiss, J., Richeton, T., Louchet, F., Chmelik, F., Dobron, P., Entemeyer, D., Lebyodkin, M., Lebedkina, T., Fressengeas, C. and McDonald, R. J. (2007). Evidence for universal intermittent crystal plasticity from acoustic emission and high-resolution extensometry experiments. *Physical Review B*, Vol.76, No.22, (Dec), pp. 1098-0121

Xia, K. N. and Langdon, T. G. (1994). The thoughening and strengthening of ceramic materials through discontinuous reinforcement. *J Mat. Sci.*, Vol.29, No.20, (Oct), pp. (5219-5231), 0022-2461

Yoo, M. H. (1981). Slip, twinning and fracture in hexagonal closed packed metals. *Metall. Trans. A*, Vol.12, No.3, pp. (409-418), 0360-2133

Yoshinaga, H. and Horiuchi, R. (1964). On nonbasal slip in magnesium crystals. *Trans. JIM*, Vol.5, No.1, pp. (14-21), 0021-4434

Yoshinaga, H., Obara, T. and Morozumi, S. (1973). Twinning deformation in magnesium compressed along c-axis. *Mater. Sci. Eng.*, Vol.12, No.5-6, pp. (255-264), 0025-5416

Zaiser, M. (2006). Scale invariance in plastic flow of crystalline solids. *Adv. Phys.*, Vol.55, No.1-2, (Jan-Apr), pp. (185-245), 0001-8732

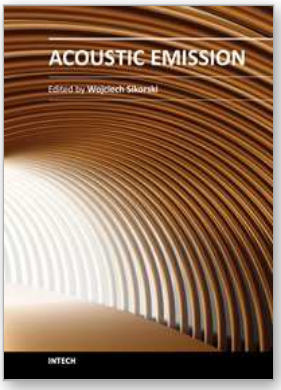

Acoustic Emission
Edited by Dr. Wojciech Sikorski

ISBN 978-953-51-0056-0
Hard cover, 398 pages
Publisher InTech
Published online 02, March, 2012
Published in print edition March, 2012

Acoustic emission (AE) is one of the most important non-destructive testing (NDT) methods for materials, constructions and machines. Acoustic emission is defined as the transient elastic energy that is spontaneously released when materials undergo deformation, fracture, or both. This interdisciplinary book consists of 17 chapters, which widely discuss the most important applications of AE method as machinery and civil structures condition assessment, fatigue and fracture materials research, detection of material defects and deformations, diagnostics of cutting tools and machine cutting process, monitoring of stress and ageing in materials, research, chemical reactions and phase transitions research, and earthquake prediction.

InTech Europe
University Campus STeP Ri
Slavka Krautzeka 83/A
51000 Rijeka, Croatia
Phone: +385 (51) 770 447
Fax: +385 (51) 686 166
www.intechopen.com

InTech China
Unit 405, Office Block, Hotel Equatorial Shanghai
No.65, Yan An Road (West), Shanghai, 200040, China
中国上海市延安西路65号上海国际贵都大饭店办公楼405单元
Phone: +86-21-62489820
Fax: +86-21-62489821